INTERNATIONAL JOURNAL OF
ENERGY AND ENVIRONMENT

*Volume 5, Issue 3, 2014 pp.361-374*

*Journal homepage: www.IJEE.IEEFoundation.org*

# Effect of the number and area of channels on the performance of rectangular, triangular and elliptical channel geometry PEM fuel cells

**I. Khazaee**

Department of Mechanical Engineering, Torbat-e-jam branch, Islamic Azad University, Torbat-e-jam, Iran.

**Abstract**
The performance of a PEM fuel cell is an important parameter that can be expressed with the polarization curve of it. In this study a complete three-dimensional and single phase model is used to investigate the effect of increasing the number of serpentine channels in the bipolar plates and also increasing the area (depth) of channels of a PEM fuel cell with rectangular, triangular and elliptical cross-section geometry. The proposed model is a full cell model, which includes all the parts of the PEM fuel cell, flow channels, gas diffusion electrodes, catalyst layers and the membrane. The results show that there are good agreement with the numerical results and experimental results of the previous work of authors. Also the results show that by increasing the number of channels from one to four and eight, the performance improved about 18% and by decreasing the area of channels from $2mm^2$ to $1mm^2$ the performance improved about 13%.


**Keywords:** PEM fuel cell; Elliptical channel; Rectangular channel; Numerical modeling; Current density.

## 1. Introduction

The polymer exchange membrane fuel cell (PEMFC) is considered to be the most promising candidate for electric vehicles by virtue of its high power density, zero pollution, low operating temperature, quick start-up capability and long lifetime. PEMFC can also be used in distributed power systems, submarines, and aerospace applications [1].
The single-cell PEMFC consists of a carbon plate, a gas diffusion layer (GDL), a catalyst layer, for each of the anode and the cathode sides, as well as a PEM membrane at the center that is shown in Figure 1.
Flow channel geometry is of critical importance for the performance of fuel cells containing proton exchange membranes (PEM) but is of less concern for solid oxide fuel cells (SOFC). The reactants, as well as the products, are transported to and from the cell through flow channels. Flow field configurations, including parallel, serpentine, interdigitated, and other combined versions, have been developed.
The performance of the fuel cell system is characterized by current-voltage curve *(i.e. polarization curve).* The difference between the open circuit potential of the electrochemical reaction and cell voltage occurs from the losses associated with the operation. The corresponding voltage drop is generally

classified in three parts: (i) activation over-potential caused by the electrochemical reactions, (ii) ohmic drop across the polymer electrolyte, (iii) mass transfer limitations of reactants.

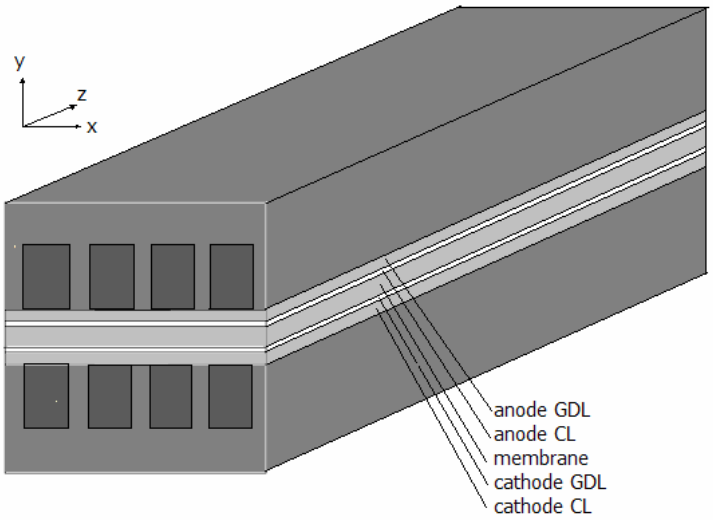


Figure 1. Schematic of a PEMFC

These associated losses dominate over different current density ranges. For low current densities; the activation over-potential is dominant. For high current densities, which are of particular interest for vehicle applications because of higher power density; the mass transfer limitations dominates the losses. For moderate current densities, the ohmic drop across the polymer membrane dominates.

Khazaee [2] investigated numerically the effect of using different obstacles on the performances, current density and gas concentration for different Aspect Ratios and compared the results with experimental results of a triangular channel geometry PEM fuel cell. He found that by increasing the hydrogen flow rate from 0.3 L/min to 0.7 L/min and the oxygen flow rate from 0.5 L/min to 0.9 L/min the cell performance enhances. Also he found that by increasing the number of the blocks in the channels and installation of rectangular block, the overall cell performance increases.

West and Fuller [3] proposed a two-dimensional numerical analysis of the rib spacing in PEM electrode assemblies on current and water distribution within the cell. The results indicated that increasing the rib width strongly affected the membrane water content before the catalyst utilization is reduced. Therefore, the two-dimensional effect has a significant influence on water management. Chiang and Chu [4] investigated the effects of transport components on the transport phenomena and performance of PEM fuel cells by using a three-dimensional model. The impacts of channel aspect ratio (AR) and GDL thickness were examined. It was found that a flat channel with a small AR or a thin GDL generates more current at low cell voltage due to the merits of better reactant gas transport and liquid water delivery. Wang et al. [5] developed a two-dimensional numerical model to study the two-phase flow transport in the air cathode of a PEMFC. In this paper, the model encompassed both single- and two-phase regimes corresponding to low and high current densities and was capable of predicting the transition between the two regimes. Jenn-Kun Kuo et al. [6] performed numerical simulations to evaluate the convective heat transfer performance and velocity flow characteristics of the gas flow channel design to enhance the performance of proton exchange membrane fuel cells (PEMFCs). Their study has simulated low Reynolds number laminar flow in the gas flow channel of a PEMFC. The heat transfer performance and enhanced gas flow velocity characteristics of four different channel geometries have been considered, namely a conventional straight gas flow channel and a gas flow channel with the three novel periodic patterns geometries. The results indicated that, compared to the conventional gas flow channel, the novel gas flow channels proposed in this study provide a significantly improved convective heat transfer performance and a higher gas flow velocity and, hence, an improved catalysis reaction performance in the catalyst layer. Khazaee et al. [7-9] proposed A complete three-dimensional and single phase model for annular-shaped and duct-shaped proton exchange membrane (PEM) fuel cell to investigate the effect of using different connections between bipolar plate and gas diffusion layer on the performances, current density, and temperature and gas concentration. They found that that the cell performance is increased as

 

the number of connections between GDL and bipolar plate increases but for one connection conditions the effect of changing the location of connection on cell performance is negligibly small. Also they found that the water mole fraction gradually increases along the cell and the maximum of it is near the connections between GDL and bipolar plate. Yan et al. [10] developed a two-dimensional mass transport model to investigate the anode gas flow channel cross section and GDL porosity effects. They found that an increase in either the GDL porosity, channel width fraction, or the number of channels could lead to better cell performance. Chu et al. [11] also used a half-cell model to investigate the effect of the change of the GDL on the performance of a PEMFC. They found that a fuel cell embedded with a GDL with a larger averaged porosity will consume a greater amount of oxygen, so that a higher current density is generated and a better fuel cell performance is obtained.

This study numerically investigated the effect of changing the number of channels and the area of channels on cell performance of a PEM fuel cell with different cross-section geometry of channels. The objective of the current work is to show the effect of changing channel geometry that it may be of interest to engineers attempting to develop the optimization of a PEMFC and to researchers interested in the flow modification aspects of the PEMFC performance enhancement.

## 2. Numerical model

The numerical model for the fuel cell used here includes the anode flow channels, anode gas diffusion layer, anode catalyst layer, proton exchange membrane, cathode catalyst layer, cathode gas diffusion layer, and cathode flow channels. The thickness of the gas diffusion layer is 0.33mm thick, the catalyst layer is 0.01mm thick, and the proton exchange membrane is 0.051mm thick. Miniature fuel cells with dimensions of $45 \times 95 \times 101\ mm^3$ with an active area of $25\ cm^2$ and serpentine and rectangular, triangular and elliptical flow field geometries of channels are considered in this investigation. For one serpentine channel the width and depth were selected to be 4 and 1.27 mm for elliptical channel, 4 and 1 mm for rectangular channel and 4 and 2 mm for triangular channel and for four serpentine channels the width and depth were selected to be 1 and 1.27 mm for elliptical channel, 1 and 1 mm for rectangular channel and 1 and 2 mm for triangular channel and for eight serpentine channels the width and depth were selected to be 0.5 and 1.27 mm for elliptical channel, 0.5 and 1 mm for rectangular channel and 0.5 and 2 mm for triangular channel respectively.

Also when the cross section area of one channel changes from $1mm^2$ to $1.5mm^2$ and $2mm^2$ only for four serpentine channels, the width and depth were selected to be 1 and 1.93 mm for elliptical channel, 1 and 1.5 mm for rectangular channel and 1 and 3 mm for triangular channel geometry and 1 and 2.55 mm for elliptical channel, 1 and 2 mm for rectangular channel and 1 and 4 mm for triangular channel respectively. The geometry of cells and channels are shown in Figure 2.

The proposed model does not require any internal boundary conditions between the components of PEM Fuel Cell system. The different physical properties and transport parameters are incorporated into a single set of governing equations using a single domain formulation. The model aims to study the electrochemical kinetics, current distribution, reactant flow fields and multi-component transport of oxidizer and fuel streams in a multi-dimensional domain. The assumptions made in developing the model are as follows:

- Ideal gas mixtures
- Incompressible and Laminar flow because low flow velocities and low fuel utilization
- Isotropic and homogeneous porous electrodes, catalyst layers and membrane
- Negligible ohmic resistance at porous electrodes and current collectors

The model assumes that the system is steady; the inlet reactants are ideal gases; the flow is laminar; and the porous layers such as the diffusion layer, catalyst layer and PEM are isotropic. The model includes continuity, momentum and species equations for gaseous species, liquid water transport equations in the channels, gas diffusion layers, and catalyst layers, water transport equation in the membrane, electron and proton transport equations. The Bulter–Volumer equation was used to describe electrochemical reactions in the catalyst layers.

The conservation equations of mass, momentum, energy, species and charge are as follows:

$$\frac{\partial(\rho\varepsilon)}{\partial t} + \nabla.(\varepsilon\rho\vec{u}) = 0 \tag{1}$$

 

$$\frac{\partial(\rho\varepsilon\vec{u})}{\partial t}+\nabla.(\varepsilon\rho\vec{u}\vec{u})=-\varepsilon\nabla p+\nabla.(\varepsilon\mu\nabla\vec{u})+S_u \tag{2}$$

$$\frac{\partial(\rho\vec{u}(E+p))}{\partial t}+\nabla.((E+p)\rho\vec{u}\vec{u})=\nabla.\left(\lambda_{eff}\nabla T-\sum_k h_k J_k+(\tau_{eff}.\vec{u})\right)+S_h \tag{3}$$

$$\frac{\partial(\varepsilon X_k)}{\partial t}+\nabla.(\varepsilon\vec{u}X_k)=\nabla.(D_k^{eff}\nabla X_k)+S_k \tag{4}$$

$$\nabla.(\sigma_g^{eff}\nabla\phi_e)+S_\phi=0 \tag{5}$$

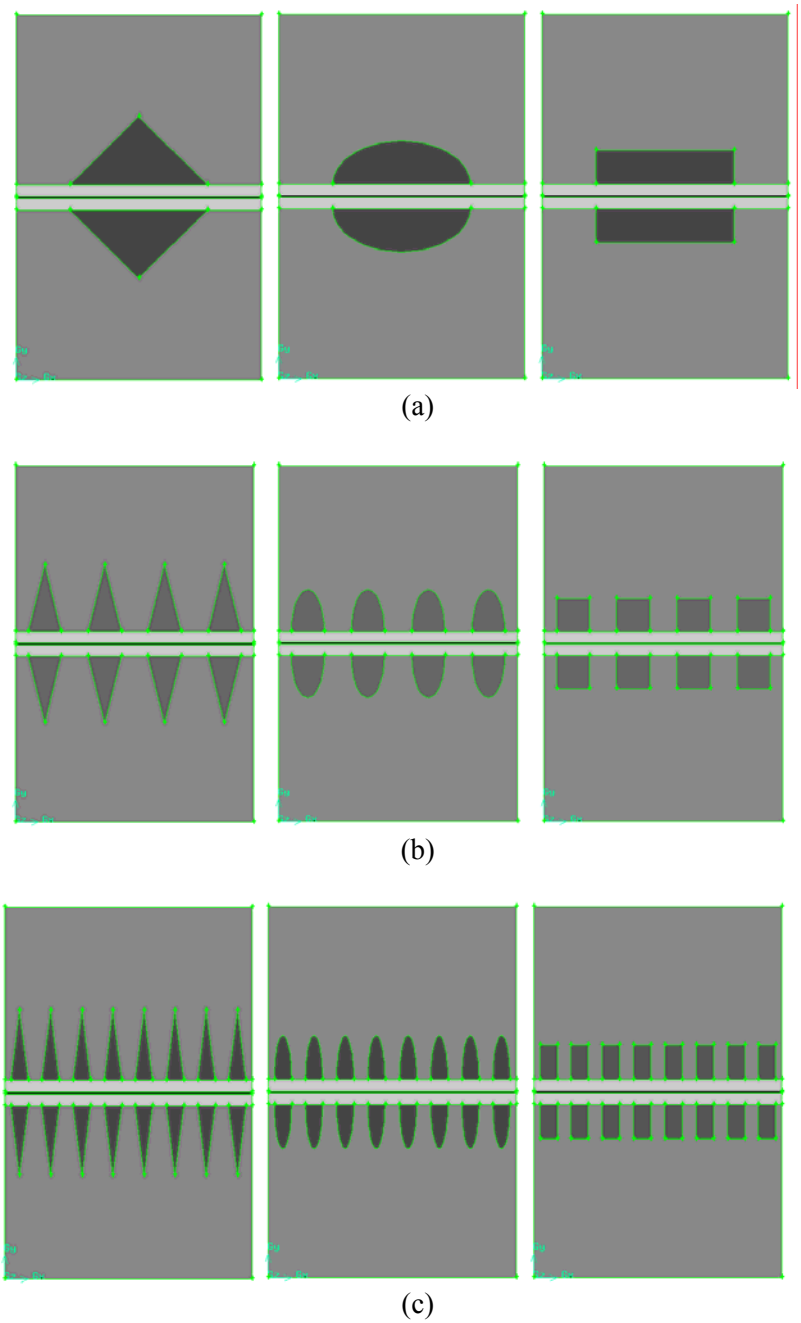

(a)

(b)

(c)

Figure 2. (a) Schematic of the one serpentine channel, (b) Schematic of the four serpentine channels, (c) Schematic of the eight serpentine channels

 

The corresponding source terms treating the electrochemical reactions and porous media are presented in Table 1.

Table 1. Source terms

| | $S_v$ (Momentum) | $S_k$ (Species) | SØ (Phase potential) | $S_h$ (Energy) |
|---|---|---|---|---|
| Gas channels | 0 | 0 | 0 | 0 |
| Backing layers | $-\frac{\mu}{k}\varepsilon^2\vec{u}$ | 0 | 0 | 0 |
| Catalyst layers | $-\frac{\mu}{k_p}\varepsilon_m\varepsilon_{mc}\vec{u}-\frac{k_\phi}{k_p}c_f F\nabla\phi$ | $-\frac{j_a}{2F}\frac{\rho}{\varepsilon_m\varepsilon_{mc}}$ : anode $H_2$<br>$\frac{j_c}{2F}\frac{\rho}{\varepsilon_m\varepsilon_{mc}}$ : cathode $O_2$<br>$-\frac{j_c}{F}\left(\frac{1}{2}+n_d\right)\frac{\rho}{\varepsilon_m\varepsilon_{mc}}$ : cathode $H_2O$<br>$-\frac{n_d}{F}j_a\frac{\rho}{\varepsilon_m\varepsilon_{mc}}$ : anode $H_2O$ | j | $\frac{\lvert j_c\rvert}{2F}T\lvert\Delta s\rvert+\lvert j_c\eta_c\rvert$ for cathode<br>0 for anode |
| Membrane | $-\frac{\mu}{k_p}\varepsilon_m\vec{u}-\frac{k_\phi}{k_p}c_f F\nabla\phi$ | 0 | 0 | $\frac{I^2}{\sigma_{mem}}$ |

$$\lambda_{eff}=\varepsilon\lambda_f+(1-\varepsilon)\lambda_s \tag{6}$$

where $\lambda_s$ is the thermal conductivity of the electrode solid matrix and $\lambda_f$ is the thermal conductivity of the gas, which can be expressed as a function of temperature:

$$\lambda_f=a_0+a_1T+a_2T^2+a_3T^3 \tag{7}$$

It is of benefit to further explain the corresponding diffusivities of the governing equations. The diffusivities for species concentration equations and ionic conductivity for membrane phase potential equation are modified using Bruggman correlation to account for porous electrodes, which can be expressed as:

$$D_k^{eff}=\varepsilon_m^{1.5}D_k \tag{8}$$

$$\sigma_e^{eff}=\varepsilon_m^{1.5}\sigma_e \tag{9}$$

It is worth further explaining the mole fraction of oxygen appearing in Eq. 4 because oxygen is a gaseous species in the cathode flow channel and gas-diffusion electrode but becomes a species dissolved in the electrolyte in the catalyst layer and membrane regions. Our definition is given by

$$X_k=\begin{cases}C_k^g/C_{tot} & in\ gas\\ C_k^e/C_{tot} & in\ electrode\end{cases} \tag{10}$$

where $C_k$ is the molar concentration of species k and superscripts g and e denote the gas and the electrolyte phases, respectively. Thus, $X_k$ is a true mole fraction in the gas phase but is a pseudo mole

 

fraction when species k is in the dissolved form. In addition, there is a discontinuity in the value of $X_k$ at the interface between the gas-diffusion electrode and the catalyst layer due to the following thermodynamic relation

$$C_k^{e,sat} = \frac{RT}{H} C_k^g \tag{11}$$

where $H$ is the Henry's law constant equal to $2\times10^5$ $atm\ cm^3 / mol$ for oxygen in the membrane.
Either generation or consumption of chemical species k and the creation of electric current occurs only in the active catalyst layers where electrochemical reactions take place. The $S_k$ and $S_\phi$ terms are therefore related to the transfer current between the solid matrix and the membrane phase inside each of the catalyst layers. These transfer currents at anode and cathode can be expressed as follows:

$$j_a = aj_{0,a}^{ref}\left(\frac{X_{H_2}}{X_{H_2,ref}}\right)^{1/2}\left(\exp\left(\frac{\alpha_a^a F}{RT}\eta_a\right) - \exp\left(-\frac{\alpha_c^a F}{RT}\eta_a\right)\right) \tag{12}$$

$$j_c = aj_{0,c}^{ref}\left(\frac{X_{O_2}}{X_{O_2,ref}}\right)\left(\exp\left(\frac{\alpha_a^c F}{RT}\eta_c\right) - \exp\left(-\frac{\alpha_c^c F}{RT}\eta_c\right)\right) \tag{13}$$

The above kinetics expressions are derived from the general Butler- Volmer equation based on the facts that the anode exhibits fast electrokinetics and hence a low surface overpotential to justify a linear kinetic rate equation, and that the cathode has relatively slow kinetics to be adequately described by the Tafel equation. In Eq. 12 and 13, the surface overpotential, $\eta(x, y)$, is defined as:

$$\eta(x,y) = \phi_s - \phi_e - V_{oc} \tag{14}$$

where $\phi_s$ and $\phi_e$ stand for the potentials of the electronically conductive solid matrix and electrolyte, respectively, at the electrode electrolyte interface. $V_{oc}$ is equal to zero on the anode but is a function of temperature on the cathode namely

$$V_{oc} = 0.0025T + 0.2329 \tag{15}$$

where $T$ is in Kelvin and $V_{oc}$ is in volts. Notice that $V_{oc}$ is not the true open-circuit potential of an electrode, which would then depend upon reactant concentrations according to the Nernst equation.
The proton conductivity in the membrane phase has been correlated as

$$\sigma_e(T) = 100\exp\left[1268\left(\frac{1}{303} - \frac{1}{T}\right)\right](0.005139\xi - 0.00326) \tag{16}$$

where the water content in the membrane, $\xi$, depends on the water activity, $a$, according to the following fit of the experimental data

$$\xi = \begin{cases} 0.043 + 17.18a - 39.85a^2 + 36a^3 & 0 \prec a \le 1 \\ 14 + 1.4(a-1) & 1 \le a \le 3 \end{cases} \tag{17}$$

The water activity is in turn calculated by

 

$$a = \frac{X_{H_2O}\, p}{p_{sat}} \tag{18}$$

where the saturation pressure of water vapor can be computed from the following empirical equation

$$\ln(p^{sat}) = 70.43464 - \frac{7362.698}{T} + 0.006952T \ - 9\ln(T\ ) \tag{19}$$

In a fuel cell system, the inlet flow rates are generally expressed as stoichiometric ratios of inlet streams based on a reference current density. The stoichiometric ratios inlet streams are given by the following equations [1].

$$S^{anode} = C_{H_2} v^{anode} \frac{2F}{I_{ref} A} \tag{20}$$

$$S^{cathode} = C_{O_2} v^{cathode} \frac{4F}{I_{ref} A} \tag{21}$$

Water transport through the polymer electrolyte membrane has been investigated by several researchers in different aspects. Most interesting studies in this area includes the determination of water diffusion coefficient and water drag coefficient by Zawodzinski et al. [12, 13] and investigating the diffusion of water in Nafion membranes by Motupally et al. [14].

The electro-osmotic drag coefficient is defined as the number of water molecules transported by each hydrogen proton $H^+$. The electro-osmotic drag coefficient can be expressed with the following equation:

$$n_d = \frac{2.5\xi}{22} \tag{22}$$

The diffusion coefficient of water in Polymer Membrane is also highly dependent on the water content of the membrane. The relation is given as:

$$D_w^m = \begin{Bmatrix} 3.1\times10^{-7}\,\xi(\exp(0.28\xi)-1)\exp(-2346/T) & 0 \prec \xi \prec 3 \\ 4.17\times10^{-8}\,\xi(1+161\exp(-\xi))\exp(-2346/T) & otherwise \end{Bmatrix} \tag{23}$$

Once the electrolyte phase potential is determined in the membrane, the local current density along the axial direction can be calculated as follows

$$I(y) = -\sigma_e^{eff} \frac{\partial \phi_e}{\partial x}\bigg| x = I.F. \tag{24}$$

where I.F. means the interface between the membrane and cathode catalyst layer. The average current density is then determined by

$$I_{avg} = \frac{1}{L}\int_0^L I(y)dy \tag{25}$$

where $L$ is the cell length.

There are natural boundary conditions of zero-flux prescribed everywhere other than the inlet and outlets of the flow channels. The boundary conditions prescribed at the inlets of the gas channels are:

 

$$u_{in}^{anode} = u_a^0 \qquad u_{in}^{cathode} = u_c^0$$
$$C_{H_2}^{anode,in} = C_{H_2}^0 \qquad C_{O_2}^{cathode,in} = C_{O_2}^0$$
$$C_{H_2O}^{anode,in} = C_{H_2O}^{0,a} \qquad C_{H_2O}^{cathode,in} = C_{H_2O}^{0,c}$$

A mesh of 325584 nods for rectangular channel, 293056 nods for triangular channel and 274360 nods was found to provide required spatial resolution for different channel geometry. The solution is considered to be converged when the difference between successive iterations is less than $10^{-7}$ for all variables.

The Electrochemical and Transport Parameters used in these simulations are summarized in Table2, and the operational parameters are presented in Table3.

Table 2. Electrochemical and transport properties

| | | |
|---|---|---|
| Anode reference exchange current density | $A/m^3$ | 1500000000 |
| Cathode reference exchange current density | $A/m^3$ | 4000000 |
| Anode transfer coefficient | | 2 |
| Cathode transfer coefficient | | 2 |
| Faraday constant | C/mol | 96487 |
| $H_2$ Diffusivity | $m^2/s$ | 0.00003 |
| $O_2$ Diffusivity | $m^2/s$ | 0.00003 |
| $H_2O$ Diffusivity at anode | $m^2/s$ | 0.00003 |
| $H_2O$ Diffusivity at cathode | $m^2/s$ | 0.00003 |
| Anode backing layer porosity | | 0.5 |
| Cathode backing layer porosity | | 0.5 |
| Permeability of anode backing layer | $m^2$ | 0.000000000001 |
| Permeability of cathode backing layer | $m^2$ | 0.000000000001 |
| Equivalent weight of membrane | kg/mol | 1.1 |

Table 3. Operational parameters

| Description | Unit | Value |
|---|---|---|
| Reference average current density | $A/cm^2$ | 1.0 |
| Oxygen flow rate | L/min | 0.5 |
| Hydrogen flow rate | L/min | 0.3 |
| Anode inlet pressure | Atm | 1 |
| Cathode inlet pressure | Atm | 1 |
| Cell temperature | C° | 60 |
| Anode inlet molar concentration | | |
| Hydrogen | $mol/m^3$ | 35.667 |
| Oxygen | $mol/m^3$ | 0 |
| Water vapor | $mol/m^3$ | 16.121 |
| Cathode inlet molar concentration | | |
| Hydrogen | $mol/m^3$ | 0 |
| Oxygen | $mol/m^3$ | 7.51 |
| Water vapor | $mol/m^3$ | 16.121 |

## 3. Results and discussion

In order to show that the program in this study can handle the cell performance of a PEMFC, we apply the present method to solve the whole of a PEMFC as described in previous section and compare it with the experimental results of authors [2].

Figure 3 show the comparison between experimental [2] and numerical results to investigate the influence of the internal flow modification on the overall fuel cell performance for three channel geometries of rectangular, triangular and elliptical shape for $T_{cell} = 60^\circ C$,

 

$T_{O2} = 55^{\circ}C, T_{H2} = 55^{\circ}C, \dot{m}_{O2} = 0.5L/\min$, $\dot{m}_{H2} = 0.3L/\min$ and P=2.905 bar. It is clear that there are good agreements between experimental and numerical results. Also it is clear that for whole operating voltage conditions the effect of the internal flow modification on the polarization curves is important that the overall fuel cell performance is at higher value when the geometry of the channel is rectangular but when the geometry of the channels shift to triangular and elliptical, the cell performance decreases that this is due to diffusing the more efficient fuel to gas diffusion layer and increasing the chemical reaction at the catalyst layer surface.

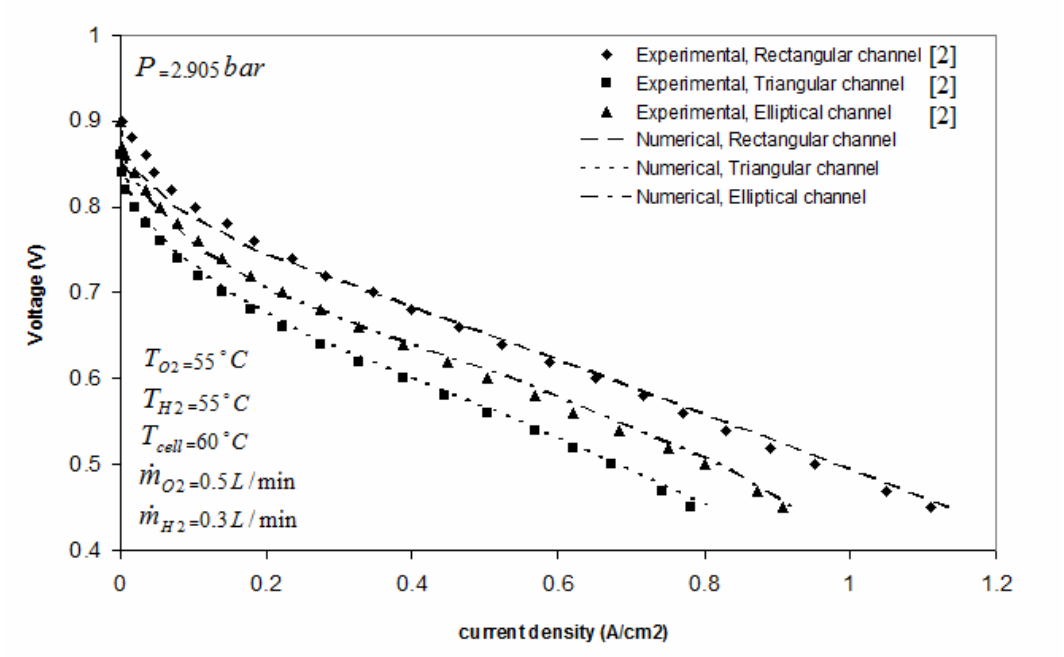


Figure 3. Comparison of numerical and experimental [2] results for three different channels for $T_{cell} = 60^{\circ}C$, $\dot{m}_{O2} = 0.5L/\min$, $\dot{m}_{H2} = 0.3L/\min$, P=2.905 bar, $T_{O2} = 55^{\circ}C$ and $T_{H2} = 55^{\circ}C$

Figure 4 and Figure 5 show the comparison between experimental [2] and numerical results to investigate the effect of hydrogen flow rate and oxygen flow rate of the anode and cathode sides at the overall cell performance of the PEM fuel cell for $T_{cell} = 60^{\circ}C$, $T_{O2} = 55^{\circ}C, T_{H2} = 55^{\circ}C$ and P=2.905 bar for a triangular channel geometry. It is clear that there are good agreements between experimental and numerical results. It is also clear that by increasing the hydrogen flow rate from 0.3 L/min to 0.7 L/min and the oxygen flow rate from 0.5 L/min to 0.9 L/min the cell performance enhances but when the flow rate increases from 0.7 L/min to 0.9 L/min for hydrogen and from 0.9 L/min to 1.3 L/min the cell performance decreases. It is due to that by increasing the flow rate of hydrogen and oxygen more fuel and oxidizer transport from GDL to the catalyst layer and the electrochemical reaction enhances but when the flow rate of hydrogen and oxygen increase from 0.7 L/min and 0.9 L/min the transportation of fuel and oxidizer to the GDL decrease and they come out from the channel without an electrochemical reaction.

Figures 6, 7 and 8 show the effect of the number of channels on the performance of a rectangular, triangular and elliptical cross-section channel geometry PEM fuel cell at $T_{cell} = 60^{\circ}C$, $T_{O2} = 55^{\circ}C, T_{H2} = 55^{\circ}C, \dot{m}_{O2} = 0.5L/\min$, $\dot{m}_{H2} = 0.3L/\min$ and P=2.905 bar. It is clear that at the conditions of the higher operating voltage (lower over potential), the influence of the internal flow modification on the overall fuel cell performance is negligibly small. At lower operating voltage conditions, on the other hand, the effect of the internal flow modification on the polarization curves becomes important. Also it is clear that when the number of channels at GDL increases from one to four and eight channels, the performance of fuel cell increases about 18%, 15% and 13% for rectangular, elliptical and triangular channel geometry that this is due to better diffusion of gases to GDL and increasing the electrochemical reaction at the catalyst layers. Also it is found from this Figs. that the

 

overall fuel cell performance is at higher value when the geometry of the channel is rectangular but when the geometry of the channels shift to triangular and elliptical, the cell performance decreases that this is due to diffusing the more efficient fuel to gas diffusion layer and increasing the chemical reaction at the catalyst layer surface.

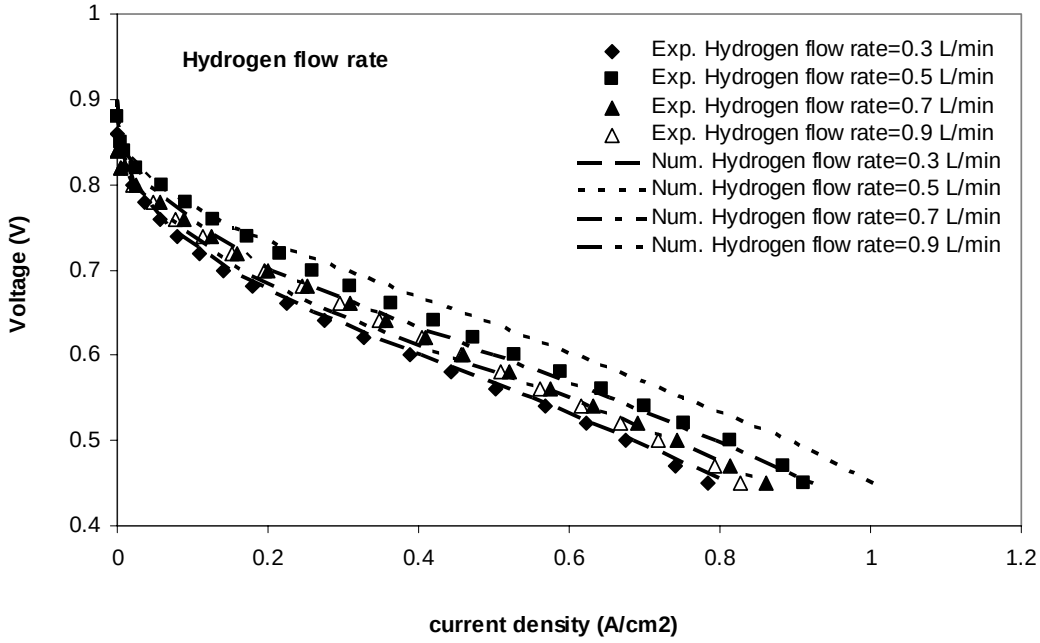


Figure 4. Variation of cell performance at different hydrogen flow rates for $T_{cell} = 60^{\circ}C$, $\dot{m}_{O2} = 0.5L/\min$, P=2.905 bar, $T_{O2} = 55^{\circ}C$ and $T_{H2} = 55^{\circ}C$

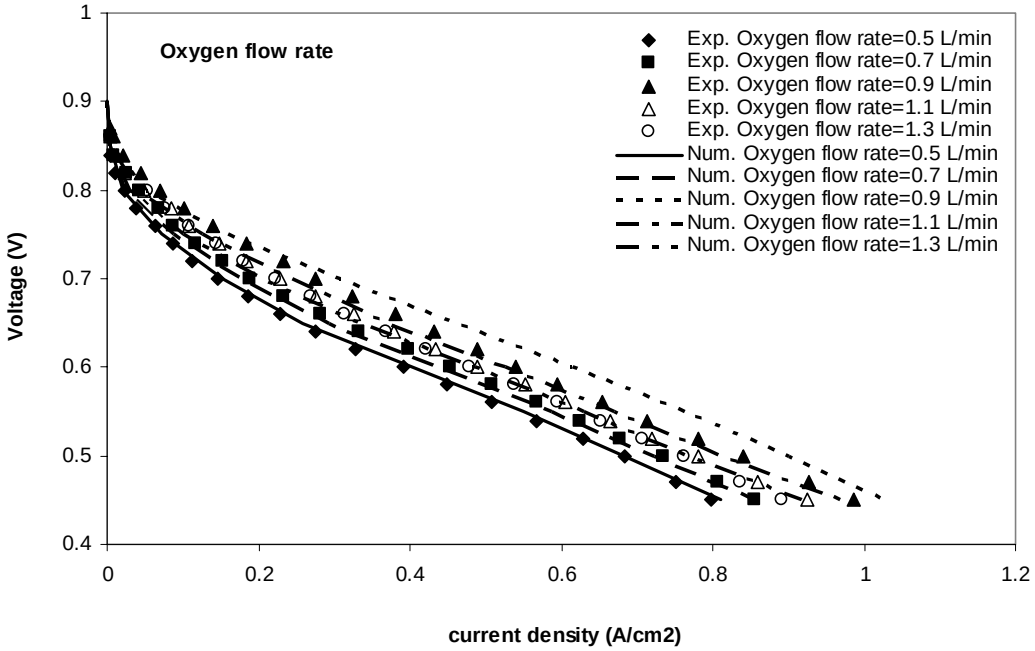


Figure 5. Variation of cell performance at different oxygen flow rates for $T_{cell} = 60^{\circ}C$, $\dot{m}_{H2} = 0.3L/\min$, P=2.905 bar, $T_{O2} = 55^{\circ}C$ and $T_{H2} = 55^{\circ}C$

 

Figures 9, 10 and 11 show the effect of the area (depth) of channels on the performance of a rectangular, triangular and elliptical cross-section channel geometry PEM fuel cell at $T_{cell} = 60^{\circ}C$, $T_{O2} = 55^{\circ}C, T_{H2} = 55^{\circ}C, \dot{m}_{O2} = 0.5L/\min$, $\dot{m}_{i2} = 0.3L/\min$ and P=2.905 bar. It is clear that at lower current density the effect of area of channels is small on the performance but at higher current density the effect of it becomes important. Also it is clear that when the area of channels increases from $1mm^2$ to $1.5mm^2$ and $2mm^2$ the performance decreases about 9%, 11% and 13% for triangular, rectangular and elliptical channel geometry that this is due to decreasing the velocity of reactant gases at the channels and decreasing the diffusion of them to the GDL and electrochemical reaction at the catalyst layer.

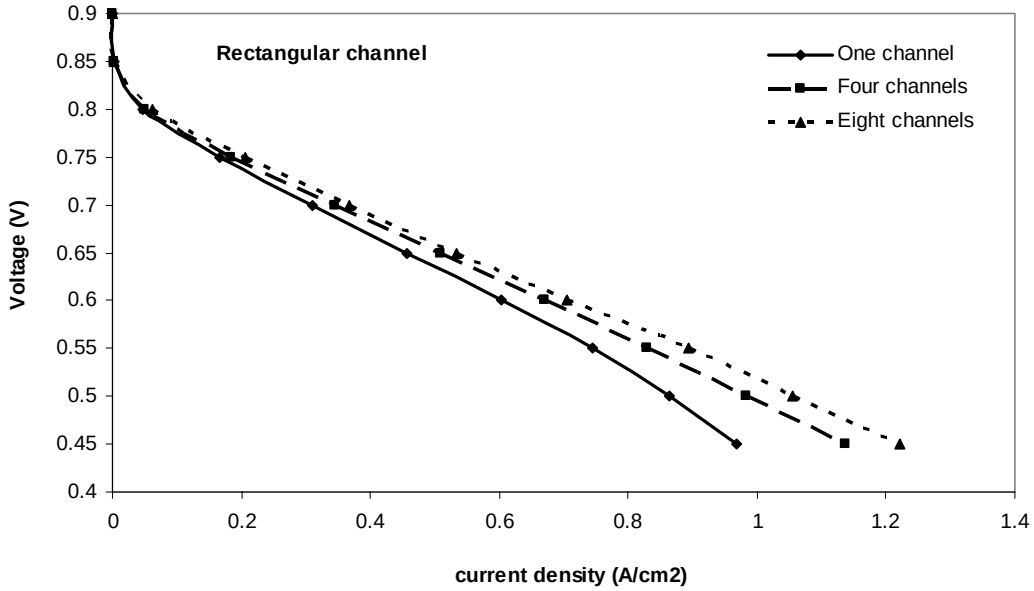


Figure 6. Effect of the number of channels on the performance for rectangular channel

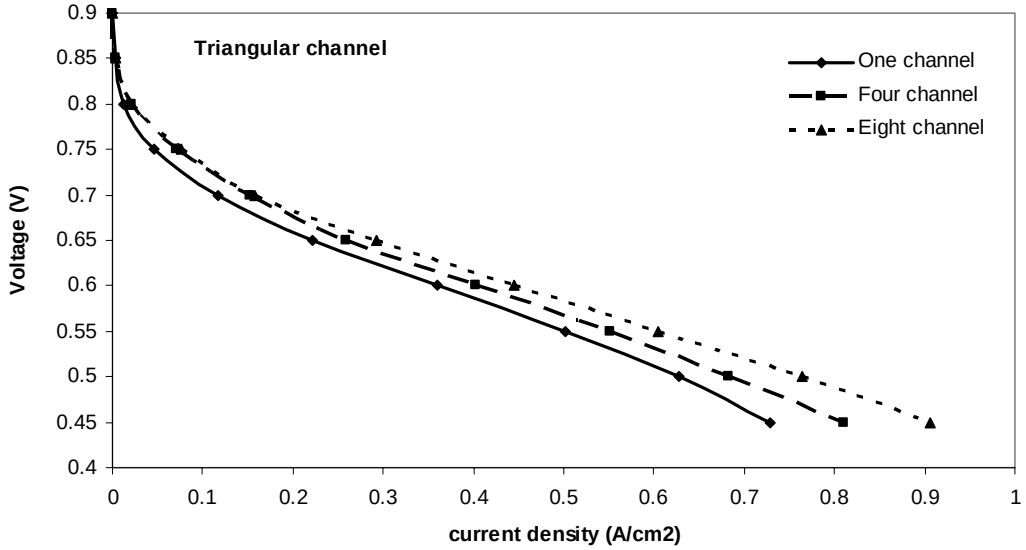


Figure 7. Effect of the number of channels on the performance for triangular channel

 

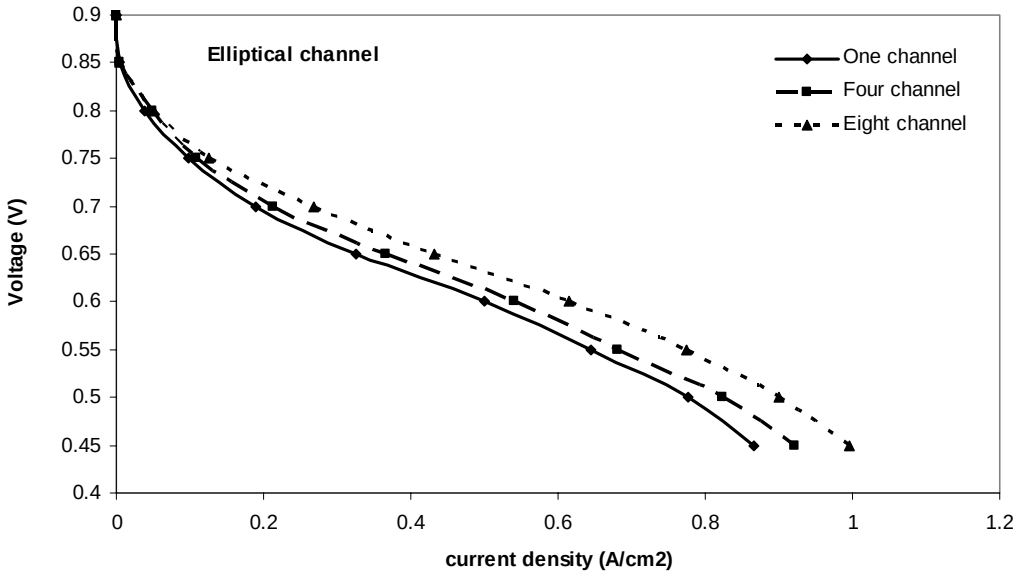


Figure 8. Effect of the number of channels on the performance for elliptical channel

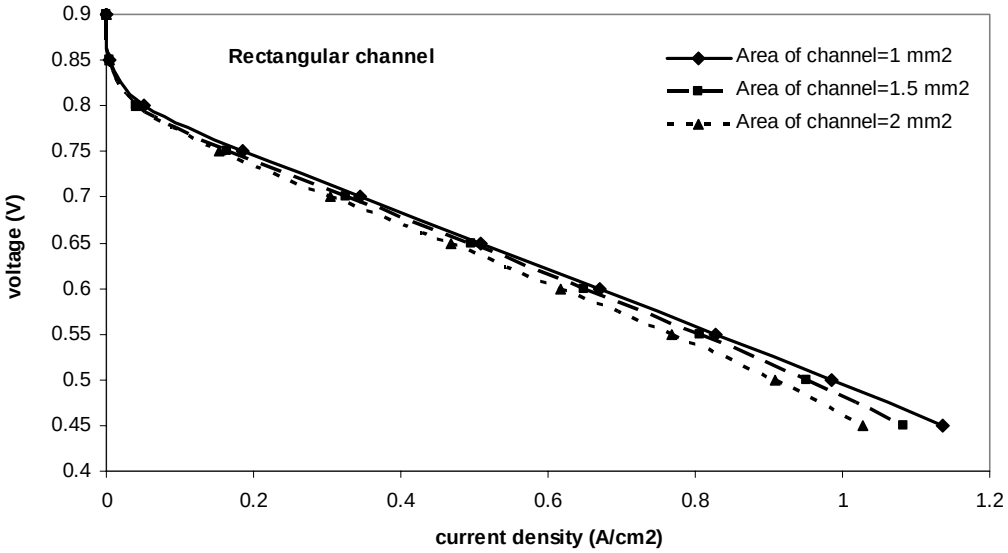


Figure 9. Effect of the area (depth) of channels on the performance for rectangular channel

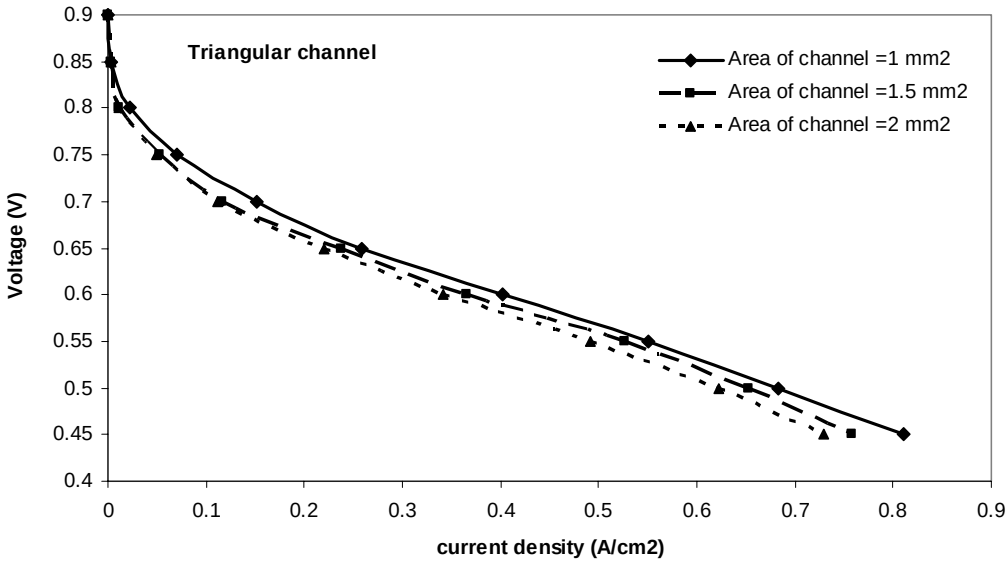


Figure 10. Effect of the area (depth) of channels on the performance for triangular channel

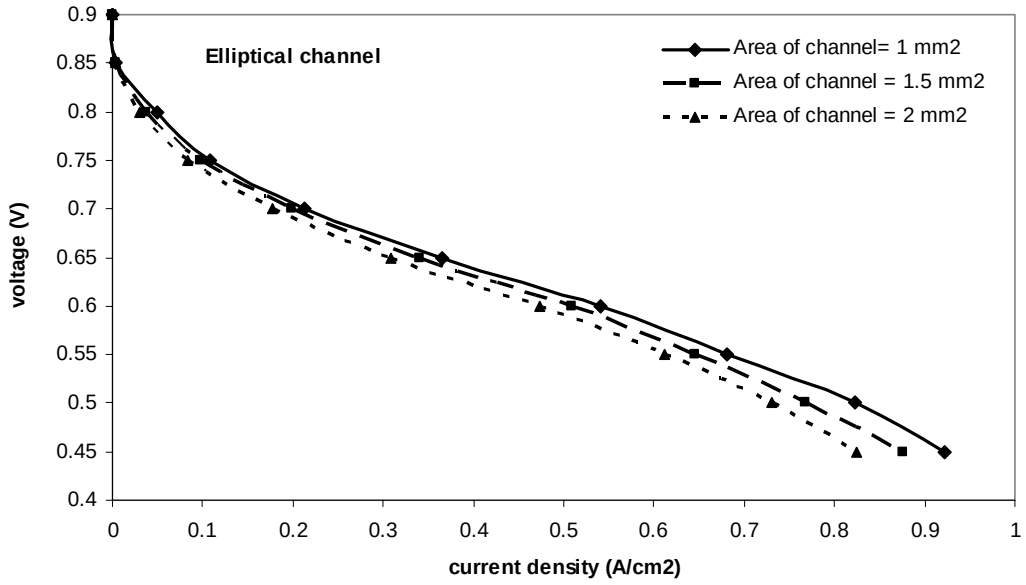


Figure 11. Effect of the area (depth) of channels on the performance for elliptical channel

## 4. Conclusion

A complete three-dimensional and single phase model for proton exchange membrane (PEM) fuel cells has been used to investigate the effect of increasing the number and cross section area of channels on the performance for three different channel geometry such as rectangular, triangular and elliptical geometry. The complete three-dimensional model for PEM fuel cells based on the two-fluid method was numerically solved with constant-temperature boundary condition at surfaces of anode and cathode current collectors. The results of this paper are in good agreement with experimental results of authors [2]. The results show that when the number of channels at GDL increases from one to four and eight channels, the performance of fuel cell increases about 18%, 15% and 13% for rectangular, elliptical and triangular channel geometry. Also the results show that when the area of channels increases from $1mm^2$ to $1.5mm^2$ and $2mm^2$ the performance decreases about 9%, 11% and 13% for triangular, rectangular and elliptical channel geometry.

## Nomenclature

| | |
|---|---|
| A | Superficial Electrode Area, $m^2$ |
| C | Molar Concentration, $mol/m^3$ |
| D | Species Diffusivity, $m^2/s$ |
| $h_k$ | Enthalpy of species k |
| I | Current Density, A/$m^2$ |
| $i_0$ | Reference current density (A/$cm^2$) |
| U | Inlet Velocity, m/s |
| j | Transfer Current Density, A/$m^3$ |
| $\vec{u}$ | Velocity vector, m/s |
| p | Pressure, Pa |
| S | Stoichiometric Ratio |
| T | Temperature, K |
| $V_{oc}$ | Reference open-circuit potential of an electrode |
| $X_k$ | Molar fraction of $k^{th}$ species |

### Greek letters

| | |
|---|---|
| $\eta$ | Overpotential, V |
| $\rho$ | density, kg/$m^3$ |
| $\varepsilon$ | porosity |
| $\sigma$ | Ionic Conductivity, S/m |
| $\phi$ | Phase Potential, V |
| $\nu$ | Volumetric Flow Rate, $m^3$/s |
| $\xi$ | Water Content of The Membrane |
| $\mu$ | Viscosity, kg m/s |
| $\alpha$ | Transfer coefficient for the reaction |
| $\tau_{eff}$ | Effective stress tensor |
| $\lambda_{eff}$ | Effective thermal conductivity in a porous material |

## Acknowledgment

This work was partially supported by Renewable Energy Organization of Iran.

 

**References**

[1] Larminie, J. and Dicks, A. "Fuel cell system explained". 2nd ed, Wiley (2003).
[2] Khazaee, I. "Effect of placing different obstacles in flow fields on performance of a PEM fuel cell: Numerical investigation and experimental comparison" Heat and Mass transfer, 49(9), pp. 1287-1298, (2013).
[3] West, A.C. and Fuller, T.F. "The Influence of Rib Spacing in Proton-Exchange Membrane Electrode Assemblies", Journal of applied electrochemistry, 26, pp 557-565 (1996).
[4] Chiang, M.S. and Chu, H.S. "Effect of placing different obstacles in flow fields on performance of a PEM fuel cell: Numerical investigation and experimental comparison Numerical investigation of transport component design effect on a proton exchange membrane fuel cell", Journal of Power Sources, 160, pp 340–352 (2006).
[5] Wang, Z.H., Wang, C.Y. and Chen, K.S. "Two-phase flow and transport in the air cathode of proton exchange membrane fuel cells", Journal of Power Sources, 94, pp 40–50 (2001).
[6] Kuo, J.K., Yen, T.S. and Chen, C.K. "Improvement of performance of gas flow channel in PEM fuel cells" Energy Conversion and Management, 49, pp 2776–2787 (2008).
[7] Khazaee, I., Ghazikhani, M."Performance improvement of proton exchange membrane fuel cell by using annular shaped geometry", Journal of Power Sources, 196, pp.2661-2668 (2011).
[8] Khazaee, I., Ghazikhani, M. and Nasr Esfahani, M. "Effect of gas diffusion layer and membrane properties in an annular proton exchange membrane fuel cell ", Applied Surface Science, 258, pp.2141-2148 (2012).
[9] Khazaee, I., Ghazikhani, M."The effect of material properties on the performance of a new geometry PEM fuel cell", Heat and Mass Transfer, 48, pp.799-807 (2012).
[10] Yan, W.M., Soong, C.Y., Chen, F.L., Chu, H.S. "Effects of flow distributor geometry and diffusion layer porosity on reactant gas transport and performance of PEM fuel cells", Journal of Power Sources, 125, pp.27-39 (2004).
[11] Chu, H.S., Yeh, C., Chen, F., "Effects of porosity change of gas diffuser on performance of proton exchange membrane fuel cell", Journal of Power Sources, 123, pp.1–9 (2003).
[12] Zawodzinski, T.A., Neeman, M., Sillerud, L.O. and Gottesfeld, S. "Determination of water diffusion coefficients in perfluorosulfonate ionomeric membranes", The Journal of Physical Chemistry, 95, pp.6040-6044 (1991).
[13] Zawodzinski, T.A., Davey, J. Valerio, J. and Gottesfeld, S. "The water content dependence of electro-osmotic drag in proton-conducting polymer electrolytes", Electrochimica Acta, 40, pp.297-302 (1995).
[14] Motupally, S., Becker, A.J. and Weidner, J.W. "Diffusion of Water through Nafion® 115 Membranes", Journal of the Electrochemical Society, 147, pp.3171-3177 (2000).

**Iman Khazaee** was born in Mashhad, Iran, in 1983. He received his B.S. degree in mechanical engineering from Ferdowsi university of Mashhad in 2006 and his master's degree at mechanical engineering department, Amirkabir University of Technology in 2008 and a PhD degree from Ferdowsi University of Mashhad in 2011. Currently, he is working on PEM fuel cells and their optimization.
E-mail address: Imankhazaee@yahoo.com

 